1    **The phosphoproteome is a first responder in tiered cellular adaptation to chemical**

2    **stress followed by proteomics and transcriptomics alteration**

3    Peiru Chen[1,2#], Yuan Li[1, 3#], Feng Xu[1#], Zhenpeng Zhang[1], Tao Zuo[1], Jiabin Guo[4], Kaixuan Li[1,2], Shu

4    Liu[1], Suzhen Li[1,5], Jian Yin[4], Lei Chang[1], Predrag Kukic[6], Mark Liddell[6], Liz Tulum[6], Paul Carmichael[6],

5    Shuangqing Peng[4], Jin Li[6*], Qiang Zhang[7#*], Ping Xu[1,2,3,5*]

6

7    [1]State Key Laboratory of Proteomics, National Center for Protein Sciences (Beijing), Research

8    and Development of New Drug of Chinese Academy of Medical Sciences, Beijing Proteome

9    Research Center, Beijing Institute of Lifeomics, Beijing 102206, China

10   [2]Hebei Province Key Lab of Research and Application on Microbial Diversity, College of Life

11   Sciences, Hebei University, Baoding 071002, China

12   [3]Department of Biomedicine, School of Medicine, Guizhou University, Guiyang 550025, China

13   [4]Evaluation and Research Centre for Toxicology, Institute of Disease Control and Prevention,

14   PLA, Beijing 100071, China; Academy of Military Medicines, Aceademy of Military Sciences,

15   Beijing 100850, China

16   [5]Anhui Medical University, Hefei 230032, China.

17   [6]Unilever Safety and Environmental Assurance Centre, Colworth Science Park, Sharnbrook,

18   Bedfordshire MK44 1LQ, UK

19   [7]Gangarosa Department of Environmental Health, Rollins School of Public Health, Emory

20   University, Atlanta, USA, GA 30322

21

22   [#]These authors contributed equally

23   **Running title: Phosphoproteome is a sensitive biomarker for cellular responses to**

24   **chemicals**

25

26   *Co-correspondence:

27   Ping Xu, 38 Science Park Road, National Center for Protein Sciences (Beijing), Changping

28  District, Beijing 102206, China.

29  Tel: 0086-10-61777113; Fax: 0086-10-61777050; E-mail: xuping@ncpsb.org.cn.

30

31  Qiang Zhang, 1518 Clifton Rd, Gangarosa Department of Environmental Health, Rollins School

32  of Public Health, Emory University, Atlanta, USA, GA 30322

33  Tel: +1 4047270154 E-mail: qiang.zhang@emory.edu

34

35  Jin Li, Colworth Science Park, Unilever Safety and Environmental Assurance Centre,

36  Sharnbrook, Bedfordshire MK44 1LQ, UK

37  Tel: +44 1234 264775; E-mail: Jin.Li@unilever.com

38

39  **Abstract**

40  Next-generation risk assessment for environmental chemicals and ingredients in consumer

41  products involves a weight of evidence (WoE) framework integrating a suite of new approach

42  methodologies (NAMs) based on points of departure (PoD) obtained from *in vitro* assays. Omics

43  techniques provide broad coverages of the molecular toxicity pathway space. Transcriptomics

44  assays especially play a leading role by providing relatively conservative PoDs in comparison

45  with apical endpoints. However, it is unclear whether and how parameters measured using other

46  omics technicquesparticipate in the cellular response to chemical perturbations, especially at

47  exposure levels below the transcriptomically defined PoD. Multi-omics coverage may provide

48  additional sensitive or confirmative biomarkers to complement and reduce the uncertainty in

49  safety decisions made using targeted and transcriptomics assays. In the present study, we

50  compared changes in transcriptomics, proteomics and phosphoproteomics with two prototype

51  compounds, coumarin, as a main study and doxorubicin, as a complementary study to

52  understand the sensitivity of the three omics techniques in response to chemically-induced

53  changes in HepG2 and AC16 cells. With measurements obtained for multiple chemical

54  concentrations and time points, we demonstrated that, compared with proteomics and

55    transcriptomics, phosphoproteomics alterations occur not only earlier in time as expected, but

56    also at much lower chemical concentrations and hence are proximal to the very early effects

57    induced by chemical exposure. The phosphoproteomics changes appear to approach maximum

58    when the transcriptomics alterations begin to be initiated. The results are consistent with a tiered

59    framework of cellular response to chemical insults, where posttranslational modification of

60    preexisting proteins is first seen before transcriptomics induction is engaged to launch a more

61    energy-expensive defense that defines a useful PoD. We conclude that as the cost becomes

62    more affordable, proteomics covering posttranslational modifications can be utilized to provide a

63    more complete coverage of chemical-induced cellular alteration and supplement

64    transcriptomics-based health safety decision making.

65

66    **Key words:** transcriptomics, proteomics, phosphoproteomics, point of departure, new approach

67    methodology

68

69    **Introduction**

70    Next-generation chemical risk assessment (NGRA) is moving steadily toward relying on cell- or

71    organoid-based assays to identify useful *in vitro* points of departure (PoD) that can be used in

72    safety decision-making[1-3]. In assayed cells, a myriad of molecular and morphological changes

73    can be induced by chemicals, depending on the physiochemical property of the chemicals, their

74    concentrations and exposure durations. Some chemicals can induce these changes through

75    recognizing specific molecular targets in the cells, such as receptors or enzymes, to activate or

76    inhibit one or multiple toxicity pathways. Alternatively, reactive chemicals, which do not

77    necessarily have a specific molecular target, can induce cellular responses via activating stress

78    pathways[4, 5]. Regardless of the nature of chemical actions, many of these induced changes can

79    be measured economically and used as biomarkers to cover a variety of specific cellular and

80    molecular endpoints, such as receptor binding, enzyme inhibition, immunomodulation, DNA

81    damage, stress responses, and mitochondrial activity[4, 6-10].

3

82    Targeted analyses focusing on a suite of specific cellular and molecular endpoints cannot

83    provide sufficient coverage of the biological space perturbed by a chemical, especially for novel

84    chemicals whose mode of actions are unknown. Yet, any apical endpoint change indicative of

85    impaired health must be underpinned by some alterations at the omics levels, including the

86    metabolome, proteome, transcriptome, epigenome and genome[11-13]. Technical advancements of

87    omics tools in the past two decades have enabled global coverage of molecular changes

88    occurring in cells that is unmatched by traditional targeted analyses. Due in a large part to the

89    relatively lower cost, broader biological coverage, higher S/N ratio, and smaller sample size,

90    transcriptomics has been at the top of the omics assay list in the past decades for examining

91    cellular response to biological and chemical perturbations. Starting with early functional

92    toxicogenomics studies using gene microarrays and followed by next-generation RNA

93    sequencing in recent years, transcriptomics has become a routine assay in toxicological

94    research *in vivo* and *in vitro*[14-16]. An increasing number of studies have revealed a consensus

95    that seems to hold across the chemical and biological space – the PoD as defined by the most

96    sensitive transcriptomics pathway alterations in short-term animal or *in vitro* cell assays appears

97    to be within a similar order of magnitude to the doses or concentrations causing pathological

98    outcomes in long-term animal studies for many legacy chemicals whose toxicities are known[17-23].

99    This concordance in PoD between transcriptional and apical endpoint changes is largely

100    conserved for both cancer and noncancer endpoints[18]. Thus, transcriptomics is emerging as one

101    of the most promising new approach methodologies (NAMs) with broad coverage for chemical

102    toxicity screening. As a result of these encouraging developments in toxicogenomics, developing

103    high-throughput transcriptomics *in vitro* assays and associated bioinformatic tools is one of the

104    top priorities in the next-decade blueprint recently launched by the US EPA[10].

105    It is becoming general practice now to use the beginning of transcriptomics alterations, often

106    defined by the benchmark dose (BMD) either at gene or pathway levels[24, 25], to provide a PoD for

107    safety assessment. The cutoff values for the number of genes or fold-change of differential

108    expression selected to determine the BMD may introduce uncertainty, along with uncertainties

109    associated with determining the BMD confidence lower limit. Beside the statistical considerations,

110    mechanistically speaking, it is not completely clear how transcriptomics alterations are linked to

111    adverse apical endpoint changes for broad classes of chemicals. Receptor-mediated or

112    target-specific transcriptomics alterations, when of sufficient magnitude and duration, can be led

113    to an alternative or compromised functional state in a cell, thus leading to potential apical

114    adversity. In comparison, reactive chemicals can elicit nonspecific adaptive cellular stress

115    responses requiring transcriptional induction of key stress genes[4]. Cellular stress responses are

116    bioenergetically demanding as a suite of stress proteins need to be synthesized *de nova* in large

117    quantities[26-31]. As a result, cells may enter a survival mode where they undergo global

118    translational and metabolic reprogramming to preserve and divert energy for the stress response

119    while specialized cell functions may be compromised[32, 33]. Therefore, the onset of adaptive

120    transcriptional stress control, for the purpose of cell survival, may be regarded as the onset of

121    functional adversity.

122    If apical adverse outcomes involve obligatory transcriptome-mediated responses, it begs the

123    question 'what are the mechanisms that protect cells from the chemical insult and preserve

124    functions under exposures below the transcriptomically-defined PoD doses?'. If known, these

125    non-transcriptomics molecular changes, occurring at lower doses, may be exploited to develop

126    sensitive biomarkers that can help reduce the uncertainty associated with PoD in a WoE safety

127    assessment framework. Many posttranscriptional control mechanisms appear to be engaged by

128    activating pre-existing stress proteins that are not activated at nonstressed conditions[5, 34]. This

129    activation can be mediated through posttranslational modifications such as phosphorylation,

130    oxidation, and acetylation[35-37]. Compared with the resource-heavy transcriptional adaptation,

131    these posttranslational processes are fast-responding and demand much less energy. Thus cells

132    are likely to cope with chemical stresses in a two-tiered manner[5]. At low concentrations, cells use

133    posttranslational regulation of pre-existing stress proteins to maintain homeostasis without

134    affecting their specialized functions as no global translational and metabolic reprogramming is

135    engaged. At higher concentrations, pre-existing stress proteins are activated and transcriptional

5

136  induction is initiated to increase their abundance to continue to maintain homeostasis and

137  survival.

138  Therefore, the transition from posttranslational to transcriptional control, where proteomics

139  changes are fully engaged and transcriptomics induction is initiated, may mark a PoD (i.e., the

140  transcriptomics PoD), where specialized cell functions begin to be compromised resulting in

141  reduced fitness. In cases where there are typically low exposures, such as environmental

142  exposure or in the situation of cosmetic usage of ingredients at low concentrations,

143  posttranslational-mediated protection may be at play. At higher exposures,

144  transcriptomically-mediated protection may have collateral adverse consequence, leading to

145  safety concerns. As a result of the two-tiered stress response, it is worth monitoring

146  posttranslational changes as additional biomarkers that can more sensitively detect and

147  corroborate the PoD that is defined by the onset of transcriptomics and functional alterations.

148  In the present study, we aim to compare cellular responses at multi-omics levels, including

149  transcriptomics, proteomics and phosphoproteomics to systemically test the two-tiered response

150  hypothesis on a global scale and ascertain whether phosphoproteomics is more sensitive in

151  response to chemical challenges. coumarin and doxorubicin were selected as our case study

152  chemicals. They represent a safe compound widely used in cosmetics and a pharmaceutical with

153  known cardiotoxicity, respectively, for which historical *in vitro* data generated in HepG2 cells, a

154  hepatocyte cell line, and AC16 cells, a human cardiomyocyte cell line exist[8, 9]. In the present

155  study, we conducted multi-concentration and multi-time point transcriptomics, proteomics and

156  phosphoproteomics studies in HepG2 and AC16 cells with these two chemicals. Our results

157  demonstrated that both concentration-wise and time-wise, phosphoproteomics is much more

158  sensitive in detecting cellular responses to chemical exposures than proteomics and

159  transcriptomics; phosphoproteomics provides unique values to an integrated

160  transcriptomics-centered multi-omics approach for toxicity testing.

161

162  **Materials and Methods**

163 **Reagents and cell strains**

164 Phospho-(Ser/Thr) Phe Antibody (9631S) was purchased from Cell Signaling Technology

165 (Danvers, MA, USA). Pan Phospho-Tyrosine Rabbit pAb (AP0905) was obtained from ABclonal

166 (Wuhan, Hubei, China). Antibodies against GAPDH (CW0100) goat anti rabbit IgG-HRP

167 (CW0103S) and goat anti-mouse IgG-HRP (CW0102) were from CoWin Biosciences (Taizhou,

168 Jiangsu, China). Acetylated trypsin [38] were from Enzyme & Spectrum (Beijing, China). Coumarin

169 (C4261-50G), phosphatase inhibitor cocktail 2 (P5726) and 3 (P0044) were purchased from

170 Sigma-Aldrich (St. Louis, MO, USA), and Doxorubicin (Adriamycin) HCl (NSC 123127) was from

171 Selleck (Houston, Texas, USA). EDTA-free protease inhibitor cocktail was from Roche (Basel,

172 Basel-Stadt, Switzerland). HepG2 was obtained from ATCC (American type culture collection,

173 Washington D.C., USA).

174 **Cell culture and treatment**

175 For the treatment with coumarin, HepG2 cells were seeded into a 10-cm petri dish containing

176 Dulbecco's Modified Eagle Medium (DMEM) supplemented with 10% fetal bovine serum (FBS),

177 100 U/mL penicillin and 100 mg/mL streptomycin at 37°C in a humidified 5% $CO_2$ atmosphere

178 incubator. Serially diluted chemicals were added on the following day without or with varied

179 concentrations (0.001, 0.01, 0.1, 1, 10, and 100 µM) of coumarin at a 10-fold increment, which

180 didn't show any detectable changes in cell count and viability in our previous study[39]. All

181 coumarin experiments were performed in triplicate. Cells were recovered after treatment for 6

182 hours and 24 hours for transcriptomics analysis, and after treatment for 10 min and 24 h for

183 proteomics and phosphoproteomics analysis. For the treatment with doxorubicin, AC16 cells,

184 were cultured using the same conditions as for HepG2 cells. AC16 cells were treated with 10 nM

185 doxorubicin for 10 min, 30 min and 6 hours before recovery for transcriptomics, proteomics and

186 phosphoproteomics analysis.

187 **Transcriptomics and data processing**

188 Approximately $1 \times 10^7$ fresh cells as described above were washed twice with ice-cold PBS then

189 scraped with PBS and centrifuged at 12,000 g for 10 min at 4 °C. Total RNA was extracted using

7

190    TRIzol reagent (Invitrogen, Carlsbad, CA, USA) and treated with RNase-free DNase I (Promega,

191    Madison, WI, USA). The concentration of RNA was measured by a NanoPhotometer

192    spectrophotometer and the quality of extracted RNA was checked with standard electrophoresis

193    for RNA as previously described[40]. RNA was randomly fragmented, and then reversely

194    transcribed to synthesize the first strand of cDNA using SmartScribe Rtase (Clontech, Mountain

195    View, CA, USA). Owing to the terminal transferase activity, (dC) 3 was added to the 5'-terminus

196    during synthesis of the first strand of cDNA. The second strand was synthesized using the

197    adapter 1 primer containing (dG) 3 at the 5'-terminus. cDNAs sized 400–500 bp were isolated

198    from 2% agarose gels after electrophoresis to generate the libraries. The libraries were further

199    amplified by PCR with Pfu polymerase (NEB, Beverly, MA, USA). All libraries were sequenced

200    with the adapter 1 primer using the Illumina HiSeq-2500. Cleaned reads were aligned to the

201    Ensemble GRCh38 reference genome with Hisat2 using strand specific parameters.

202    The value of fragments per kilobase of transcript per million mapped reads (FPKM) was used

203    to clean the data and for data quality control. We set a stringent filtering criterion of FPKM value >

204    1.0 in at least one out of all 42 samples to reduce false positives. After the genes were filtered,

205    the expressed genes and transcripts were assembled and quantified by running StringTie[41]. For

206    HepG2 cells with coumarin treatment, the differentially expressed genes for the RNA-seq data

207    were calculated with gene count value by using edgeR package. Each concentration condition

208    was compared with vehicle control. A criterion of ratio > 1.5 or < 0.67 with p value < 0.05 was

209    used as the threshold for differentially expressed genes.

210    **Protein extraction**

211    Approximately $5\times10^7$ fresh cells were washed with ice-cold PBS. Cell lysis was performed on ice

212    and sonicated for 4 min (2-s on and 4-s off, amplitude 25%) in buffer containing 9 M Urea, 10 mM

213    Tris–HCl (pH 8.0), 30 mM NaCl, 5 mM IAA, 5 mM $Na_4P_2O_7$, 100 mM $Na_2HPO_4$ (pH 8.0), 1 mM

214    NaF, 1 mM $Na_3VO_4$, 1 mM Sodium glycerophophate, 1% phosphatase inhibitor cocktail 2 & 3

215    (Sigma) and protease inhibitor cocktail. Unbroken debris was eliminated by centrifugation

216    (14,800 g) at 4 °C for 15 min, and the supernatant was collected and quantified by a gel-assisted

217   method as previously described [42].

**Protein digestion by gel-aided strategy**

219   Extracted protein samples (1 mg) of equal amount for all cells were reduced with 10 mM of

220   dithiothreitol (DTT) at 45 °C for 30 min, alkylated with 20 mM of IAA in the dark at room

221   temperature (RT) for 30 min, and cleaned by a short 10% SDS-PAGE. Each gel lane was cut into

222   approximately 1 mm$^3$ small cubes and digested with Ac-trypsin at 37 °C for 14 h to generate

223   short peptides [38, 43]. The tryptic peptides were collected with extracting buffer (5% formic acid

224   (FA)，50% acetonitrile (ACN)) and dried with a vacuum dryer. About 5% of tryptic peptides were

225   used for proteomics profiling experiments and the remaining 95% for phosphoproteomics study.

**Phosphopeptide enrichment and fractionation**

227   Tryptic peptides were desalted by reverse-phase C18 Sep-Pak extraction cartridges (Waters

228   Corporation, Milford, MA, USA). Cleaned peptides were resuspended in buffer A (1% ACN, 0.1%

229   trifluoroacetic acid) and separated into 12 fractions through a Bonna-Agela C18 column (5 µm

230   reverse-phase fused-silica, 4.6 × 250 mm column) on a RIGOL-L3000 HPLC (RIGOL, Beijing,

231   China).The phosphor-peptides in each fraction were enriched with a Ti$^{4+}$-immobilized metal ion

232   affinity chromatography (IMAC) method as previously described with slight modification[44, 45].

233   Briefly, dried peptides were dissolved in 500 µL binding buffer (80% ACN, 6% trifluoroacetic acid

234   (TFA) in ddH$_2$O) and the same volume of loading buffer (10% 500 mM NH$_4$HCO$_3$, 5% ACN in

235   ddH$_2$O) followed by addition of 25 mg Ti$^{4+}$-IMAC beads. Then, the mixed samples were vortexed

236   at RT for 30 minutes, and centrifuged at 13,000 g for 6 min. The supernatant was removed,

237   washed with washing buffer 1 (50% ACN, 6% TFA in 200 mM NaCl) once and washing buffer 2

238   (30% ACN, 0.1% TFA in ddH$_2$O) twice for 30 min. After removing the supernatants, the

239   phosphopeptides were eluted with elution buffer (10% NH3•H2O) for 15 min, and then sonicated

240   in ice water for another 15 min. The mixtures were centrifuged at 17,000 g for 6 min, and the

241   supernatant was transferred into a new tube and immediately acidified with 5% FA and

242   lyophilized before LC-MS analysis.

**LC-MS/MS**

**Total cell lysate profiling**

The enriched phoshopeptides were separated with self-packed StageTip column[46]. Tryptic peptides were resuspended in loading buffer (0.1% formic acid (FA) in ddH2O) and analyzed using an EASY-nLC 1000 ultra-performance liquid chromatography (UPLC) system (Thermo Fisher Scientific, San Jose, CA, USA) equipped with a self-packed capillary column (75 μm i.d. × 15 cm, 3 μm C18 reverse-phase fused-silica), with an 80 min nonlinear gradient at a flow rate of 600 nL/min. The gradient was composed of an increase from 5% to 12% solvent B (0.1% FA in 98% ACN) for 8 min, 12% to 24% in 46 min, 24% to 36% in 20 min, 36% to 95% in 1 min, and a final hold at 95% for the last 5 min.

The eluted peptides were ionized under high voltage (2 kV) and analyzed online using a Lumos$^{TM}$ mass spectrometer (Thermo Fisher Scientific, San Jose, CA, USA). The initial MS spectrum ($MS_1$) was analyzed over a mass range of 300–1400 Da with a resolution of 60,000 at m/z 200. The automatic gain control (AGC) was set to $5 \times 10^5$, and the maximum injection time (MIT) was 50 ms. Subsequent MS/MS spectrum ($MS_2$) was analyzed by using a data-dependent acquisition mode to search for the most intense ions within 3 s, which were detected in the Orbitrap at a resolution of 15,000 after fragmentation. For each scan, the threshold for triggering $MS_2$ was set at 5,000 counts, isolation width was 1.6 m/z, normalized collision energy (NCE) was 35%, AGC was $5 \times 10^4$, and MIT was 60 ms. Precursor ion charge-state screening was enabled and all unassigned charge states, as well as singly charged species, were rejected. The dynamic exclusion was set at 25 s to avoid repeated detection of the same precursor ions.

**Phospho-peptide profiling**

Phospho-peptide samples were dissolved in loading buffer (0.1% formic acid (FA) in ddH$_2$O) and injected onto a UPLC (Ultimate 3000, Thermo Fisher Scientific, San Jose, CA, USA) equipped with self-packed capillary column (150 μm i.d.×12 cm, 1.9 μm C18 reverse-phase fused-silica). The peptides were eluted with a 78-min nonlinear gradient at a flow rate of 600 nL/min with an elution gradient and eluted samples were analyzed by Q-Exactive HF or LUMOS (Thermo Fisher Scientific, San Jose, CA, USA) in a data-dependent acquisition (DDA) mode. Briefly, the spray

10

271  voltage was set as 2.2 kV, MS full scans were performed in the ultra-high-field Orbitrap mass

272  analyzer in range of m/z 300-1400 with a resolution of 120,000 at m/z 200, the maximum

273  injection time (MIT) was 80 ms and the automatic gain control (AGC) was set as $3×10^6$. The top

274  20 intense ions were selected and subjected to Orbitrap for further fragmentation via high energy

275  collision dissociation (HCD) activation over a mass range between m/z 200 and 2000 at a

276  resolution of 15,000 with the intensity threshold kept at $2.6×10^4$. We selected ions with charge

277  state from 2+ to 6+ for sequencing. Normalized collision energy (NCE) was set at 27. For each

278  $MS_2$ scan, the target AGC was set as $2 × 10^4$ and the MIT was 19 ms. The dynamic exclusion for

279  precursor ions were set over a time window of 12 s to suppress repeated peak fragmentation.

280  **Proteomics and Phosphoproteomics Data Processing**

281  Raw data of proteomics and phosphoproteomics were processed with MaxQuant (version

282  1.6.0.1). MS and MS/MS spectra were searched against the human Uniprot database (version

283  201506) using the Andromeda search engine. The database search was performed with the

284  following parameters: an initial mass tolerance of ±20 ppm and a final mass tolerance of ±0.5 Da

285  for precursor masses, ±0.6 Da for HCD ion trap fragment ions, and two missed cleavages

286  allowed. Cysteine carbamidomethylation was used as a fixed modification, and methionine

287  oxidation, protein N-terminal acetylation, and serine, threonine, and tyrosine phosphorylation

288  were included as variable modifications for phosphoproteomics data. The false discovery rate

289  was set at 0.01 for peptides, proteins, and phosphosites; the minimum peptide length allowed

290  was seven amino acids, and a minimum Andromeda peptide score of 60 was required. The

291  match-between-runs feature was enabled. A site localization probability of at least 0.75 and a

292  score difference of at least 5 were used as thresholds for the localization of phosphoresidues.

293  Reverse and contaminated proteins were removed after database search. Next, the proteins

294  and phosphosites with quantitative intensity values in less than 4 of the 21 samples in each time

295  point were removed. After the filtration, the quantitative protein information was median

296  standardized. Normalization was performed by subtracting the median of log transformed

297  intensities for each nano-LC-MS/MS run. Given that the data followed the normal distribution, we

298   imputed the missing values from normal distribution in Perseus software [47]. To identify

299   significantly regulated phosphorylation sites or proteins, limma package was used for HepG2 cell

300   with coumarin treatment. A fold change of > 1.5 or < 0.67 with p-value < 0.05 was used as the cut

301   off threshold for differentially expressed proteins and phosphosites. As no biological replicates

302   were included in the doxorubicin experiments on AC16 cells, we used a more stringent 2-fold

303   change for differential expression of genes/proteins/phosphosites. The Mfuzz package was used

304   to obtain the temporal trends of changes in phospho-sites.

305       KEGG enrichment analysis was analyzed and visualized in the DAVID bioinformatics database.

306   The change at a functional level in different groups was performed with reactome analysis.

307   Boxplot and PCA plots were generated using *ggplot2* [48]. A pairwise Pearson correlation

308   coefficient was calculated for all group runs in *R* v.3.6.1[49]. Different colors of sample correlation

309   analysis were used to represent different sample types in the hierarchical clustering analysis by

310   using the ward.2 method in the *pheatmap* package.

311   **Western blotting**

312   After cell treatment with the same conditions as in the proteomics study. An equal amount of total

313   protein was resolved by a 10% sodium dodecyl sulfate polyacrylamide gel (SDS-PAGE) and

314   transferred to nitrocellulose membranes (Bio-Rad, Hercules, CA, USA). Membranes were

315   blocked and incubated with either anti Phospho-(Ser/Thr) Phe Antibody (9631S) or anti

316   Phospho-Tyrosine Rabbit pAb (AP0905) primary antibodies overnight at 4 °C, then washed and

317   subsequently incubated with goat anti-mouse IgG-HRP (CW0102) secondary antibodies.

318   GAPDH was used to control the amount of proteins loaded for western blotting, in which anti

319   rabbit IgG-HRP (CW0103S) was used as the primary antibodies. The membranes were stained

320   with SuperSignal™ West Pico PLUS Chemiluminescent Substrate (34580, Thermo Fisher

321   Scientific, San Jose, CA, USA). Protein bands were visualized using Tanon-5200 (Tanon,

322   Shanghai, China).

323   **Computational modeling**

324   A minimal mathematical model of posttranslational and transcriptional stress adaptation was

12

325  constructed to illustrate the differential responses. Model parameter values and ordinary

326  differential equations (ODEs) are provided in Tables S15 and S16 respectively. The model was

327  constructed and simulated in Berkeley Madonna (version 8.3.18, University of California, Berkeley,

328  CA, USA) using the "Rosenbrock (stiff)" ODE solver. The model code was provided as supplemental

329  material.

330

331  **Result**

332  **Quality assurance of multi-omics study for cellular response to coumarin**

333  After evaluating the cellular response data for coumarin in the literature[50-52], we found that the

334  lowest $AC_{50}$ (concentration inducing the half-maximum assay response) for coumarin in HepG2

335  cells is about 30 μM (Table S1). Since it was anticipated that the proteome and phosoproteome

336  are sensitive to chemical perturbations, we decided to use a wide range of concentrations biased

337  to the lower end of 30 μM to explore the coumarin's effects at these two omics levels as well as

338  on the transcriptome. Besides the vehicle control, 6 concentrations were used in HepG2 cells

339  ranging between 0.001-100 μM at a 10-fold increment (Figure 1). This range of coumarin

340  concentrations in our previous study caused no detected changes in cell count and viability of

341  HepG2 cells[39]. In addition, we defined 0 μM as control, 0.001-0.01 μM as low-concentration,

342  0.1-1 μM as mid-concentration, and 10-100 μM as high-concentration groups. For

343  transcriptomics analysis, the cells were treated for 6 and 24 hours for each coumarin

344  concentration. For proteomics and phosphoproteomics analyses, the cells were treated for 10

345  min and 24 hours. The 10 min time point was chosen because rapid changes in the

346  phosoproteome, and possibly the proteome, are expected to occur on this time scale[53].

347  **Global differences in transcriptomics, proteomics and phosphoproteomics responses to**

348  **coumarin**

349  After the strict quality control on multi-omics data were conducted (Figures S1-4, Tables S2-6),

350  we performed PCA analysis which was considered as an initial effort to investigate which omics

351  is better at distinguishing different levels of perturbations by coumarin, we first applied principal

352    component analysis (PCA) to the datasets. For the 6 hours exposure groups in the RNAseq

353    experiment, PCA can barely separate the 21 samples treated with different concentrations of

354    coumarin, except that the three replicates treated with the highest concentration, i.e., 100 μM,

355    tended to cluster together and stayed away from the remaining samples (Figure 2A). The

356    segregation of the 100-μM samples from the rest is even more obvious in the 24 hours exposure

357    group (Figure 2B). These results are consistent with the reported AC50 values for coumarin in

358    HepG2 cells, which ranged between 28-163 μM, indicating that transcriptomics changes are

359    likely concordant with those cellular assay changes.

360       In contrast to the results obtained with transcriptomics, the proteome is better at distinguishing

361    different coumarin concentrations, especially for high and low concentrations. Even for 10 min

362    exposure, both the 10 and 100 μM samples are easily separated from the remaining

363    concentrations and the three 10 μM replicates form a cluster that can be distinguished from the

364    100 μM replicate cluster (Figure 2C). There also seems to be a better separation between the

365    middle-concentration (0.1-1 μM) and low-concentration samples (0.001-0.01 μM) of the

366    proteomics data than the transcriptomics data. Interestingly, for 24 hours exposure, the

367    high-concentration samples can no longer be easily differentiated from the middle-concentration

368    samples. However, the low-concentration group can be readily distinguished from middle and

369    high-concentration groups (Figure 2D). In addition, it is interesting to found that the results of

370    control samples were quite close to the low concentration samples which not only because of the

371    limit of detection sensitivity for mass spectrum, but may also indicate the biological significances

372    between them and turn out to be consistent with our knowledge that the biological activity of

373    low-dose of coumarin were slight[54]. Similar to the proteomics results, the phosphoproteome

374    could effectively distinguish high and low-concentration groups. For 10 min exposure to

375    coumarin, the high-concentration group stands out from the rest, and the low and

376    middle-concentration groups also seem distinguishable from each other (Figure 2E). 24 hours

377    exposure gave the clearest distinction, where all three dose groups are clearly separated on the

378    2D PC plot, and the samples treated with 0.001-0.01 μM coumarin are also distanced from the

14

379    vehicle control (Ph24h_1_x) samples (Figure 2F). In summary, the proteome and

380    phosphoproteome are much more sensitive than the transcriptome in distinguishing cellular

381    responses to coumarin exposure of different concentrations.

382        To further compare the effects of treatments with different concentrations of coumarin for

383    different exposure durations, we applied unsupervised hierarchical clustering to the dataset. For

384    short exposure duration, as expected, the transcriptomics data could not distinguish coumarin

385    concentration groups as they all are mixed together (Figure S5A). With the long exposure

386    duration, only the 100 µM coumarin group could be separated into a distinguishable cluster from

387    the rest of the concentration groups (Figure S5B). The proteome data could divide into two broad

388    clusters, one for high-concentration coumarin treatment, another for mid and low-concentration

389    coumarin treatments and control group, and the latter can be further grouped into separate

390    clusters (Figure S5C). The control and the ultra-low (0.001 µM) samples cannot be readily

391    distinguished from each other. With the exposure prolonged to 24 hours, different coumarin

392    concentration groups can still be distinguished but the separation does not seem to improve over

393    the short exposure data (Figure S5D). Similar to the PCA results, the phosphoproteome showed

394    the most distinct dose dependent separation among the three omics datasets. The replicates for

395    each coumarin concentration are always cleanly clustered together, for both the short and long

396    exposure durations. The separation and similarity between treatment groups strictly follow the

397    order of the coumarin concentrations including the control (Figure S5E&F). Taken together, the

398    hierarchical clustering results are consistent with the results from PCA analysis, further

399    confirming that the phosphoproteome could effectively distinguish the cellular responses to

400    chemical treatments at different concentrations, especially for ultra-low concentrations.

401    **Phosphoproteome is several orders of magnitude more sensitive than transcriptome in**

402    **response to coumarin**

403    To further understand the sensitivity of various omics techniques in detecting chemical

404    perturbations, volcano plots were generated to identify significantly altered mRNA, protein, and

405    phosphosite features in HepG2 cells (Figure S6). The $\log_2$ fold change of each feature in a

15

406    coumarin concentration-duration treatment group relative to control was plotted against $-\log_{10}$ of

407    the p-value for the transcriptomics, proteomics, and phosphoproteomics data, as shown in

408    Figure S6A-6C, respectively. As reflected by the widening of the volcano plots, a striking trend is

409    that the number of significantly altered features increases tremendously moving from

410    transcriptomics, to proteomics and phosphoproteomics responses (Figure 3A). As the coumarin

411    concentration increases, the numbers of significantly altered features increase, which also seem

412    to increase with longer exposure duration, especially for the mRNA data. When the numbers of

413    significantly altered features achieved by different coumarin concentrations were normalized to

414    that achieved at 100 µM, the highest coumarin concentration, each omics exhibits distinct

415    concentration-response profiles (Figure 3B&C). The transcriptome is clearly the least sensitive,

416    where a high response only takes off at >10 µM. In contrast, the phosphoproteomics response is

417    the most sensitive, already at 50% or higher at 0.001 µM coumarin for both short and long

418    exposure durations. Compared with transcriptomics and phosphoproteomics responses, the

419    sensitivity of the proteomics response falls in between.

420    **High detection sensitivity is conserved for phosphoproteomics in doxorubicin-treated**

421    **AC16 cells**

422    We next investigated whether the high sensitivity of phosphoproteomics observed for cellular

423    response to coumarin in HepG2 cells can also be recapitulated in other cell types in response to

424    other chemicals. We applied the same experimental approach to AC16 cells, a cardiomyocyte

425    cell line, treated with doxorubicin. Doxorubicin is a chemotherapeutic agent used in the treatment

426    of solid tumors and hematological malignancies. The most important dose-limiting toxicity of

427    doxorubicin is its cardiotoxicity[55]. The previously reported PoD of doxorubicin in AC16 cells was

428    125 nM, at which a variety of cellular responses were significantly altered, including

429    mitochondrial ROS, membrane potential and DNA content, and key genes involved in

430    mitochondrial biogenesis and antioxidant response[56]. Similarly, iPSC-derived cardiomyocytes

431    experienced beating changes at around 150 nM of doxorubicin treatment, which is a PoD also

432    eliciting transcriptomics changes[57]. To test the distinguishing power of different omics in detecting

16

433    perturbation by doxorubicin, we selected 10 nM as the concentration to treat AC16 cells, which is

434    at least 10-folder lower than the PoD above. The omic-level responses were measured at varied

435    exposure durations, including 10, 30 and 360 min, which covered both fast and delayed

436    responses (Figure 4A).

437    The qualities of the transcriptomics, proteomics and phosphoproteomics data of

438    doxorubicin-treated AC16 cells were very similar to those of coumarin-treated HepG2 samples

439    (Figure S7-S9, Table S7-S9). Given the high quality and the consistency of the replicates of the

440    coumarin-treated HepG2 samples, we are confident with the low variability of our

441    data-generating platform and moved forward with single replicates for the doxorubicin-treated

442    AC16 cells. After normalizing the abundance, the global signals for transcriptomics and

443    proteomics at various time points were stable compared with the control. This result is consistent

444    with the fact that the concentration of doxorubicin used here is much lower than the PoD

445    concentration and thus is not expected to elicit responses at transcriptomics and proteomics

446    levels. In contrast, in response to 10 nM doxorubicin, the abundance signal of altered

447    phosphoproteome spiked immediately to a peak level at 10 min, then decreased till 30 min, and

448    increased slightly by 360 min (Figure 4B). Probing total cell lysate with pan-antibodies against

449    pSer/pThr (pST) and pTyr, we found that anti-pST signal was increased in doxorubicin treated

450    samples compared with the control, but not pTyr (Figure 4C&D). This might result from low

451    detection sensitivity of pan-antibodies against pTyr used in this study[58, 59]. Taken together, these

452    results confirmed that phosphoproteome was more sensitive to reflect cellular response under

453    low and ultra-low concentrations of chemicals that normally do not disturb the transcriptome and

454    proteome.

455    **Potential sensitive biomarkers for cellular response to doxorubicin**

456    Finally, we asked the question whether we could find specific sensitive biomarkers in the

457    phosphoproteome as a mechanistic indicator for doxorubicin. We systematically analyzed the

458    multi-omics data generated from the doxorubicin-treated AC16 samples. By using a stringent

459    two-fold change as the threshold, we identified 695, 729 and 686 significantly up-regulated

460    phosphosites for samples treated with doxorubicin for 10, 30, and 360 min, respectively. The

461    down-regulated phosphosites were 629, 640 and 742, respectively (Figure 5A). Reactome

462    pathway analysis[60] of all up-regulated phosphosites showed that the cell cycle and mitosis

463    related pathways were significantly enriched (underlined in Figure 5B). Other altered pathways

464    include those for RNA metabolism and Rho GTPase signaling. This is consistent with the

465    observations that doxorubicin inhibited cell proliferation through cell cycle arrest at the G2/M

466    phase[61] and doxorubicin induced increases in mitotic activity in BE(2)-C neuroblastoma[62].

467    However, this cell cycle effect occurs at much lower concentrations than therapeutic

468    concentrations.

469    Time-series clustering analysis showed that a total of 194 phosphosites were upregulated

470    persistently throughout the 360-min duration of doxorubicin treatment (Figure 5C, Table S10).

471    These upregulated phosphosites correspond to 167 proteins, among which, 157 were also

472    identified in the proteome dataset (Table S11). Interestingly, 19 of the proteins form a single

473    proteomics cluster, which exhibited baseline-level responses in the first 30 min and then

474    upregulation at 6 hours (Figure 5C). In contrast, no tangible changes in the corresponding genes

475    were observed through the entire time course (Figure 5C). These results suggest that

476    upregulation of these genes only occurred at the posttranscriptional, and especially

477    posttranslational, level.

478    We next examined how some well-known doxorubicin-induced pathways behave in the three

479    omics datasets. By eliciting oxidative stress, doxorubicin can induce the antioxidant response in

480    cardiomyocytes, including the master transcription factor Nrf2 and signature target gene

481    HMOX1[8]. Although Nrf2 is activated through protein stabilization and in some cases

482    transcriptionally through autoregulation[63, 64], it was not identified in either of our omics datasets. It

483    is because the concentration of doxorubicin used is well below the PoD. In comparison, HMOX1,

484    which is a highly sensitive biomarker for antioxidant response, was identified in our proteome

485    data (Table S12). TSC2 (ser939) is an important protein that can activate p53, which mediates

486    the DNA damage response to doxorubicin[65]. TSC2 was identified in our phosphoproteomics data

487    (Table S13). All of these three known molecular markers have been identified and included in

488    these 19 proteins. These results strongly supported that phosphoproteomics is a sensitive

489    approach to assess the cellular response to doxorubicin. STQSTM1/p62 is heavily related to

490    cardiotoxicity although without any direct evidence regarding the toxicity of doxorubicin so far[66, 67].

491    The phosphorylation of p62 is controlled by CDK1 and plays biological roles in promoting cell

492    cycle initiation, mitosis and tumor proliferation[68]. p62 (Ser28) was increased about 19-fold at 10

493    min compared with control, which is consistent with the global trend of doxorubicin-induced

494    phosphoproteomics changes (Table S14). The biological function of this molecule in the cellular

495    response to doxorubicin treatment is unknown.

496    **A minimal mathematical model recapitulated tiered cross-omics responses**

497    To better interpret and understand the observed temporal and concentration-dependent

498    multi-omics response patterns, we constructed a minimal mathematical model capturing the

499    framework of tiered cross-omics cellular adaptation to stress[5, 32]. The model contains both post

500    translationally and transcriptionally-mediated negative feedbacks (Figure 6A, Table S15-16).

501    Specifically, it includes phosphorylation and thus posttranslational activation of a preexisting,

502    basal stress protein by a kinase which is activated by controlled state (such as ROS and DNA

503    damage) when perturbed by stressor (step 1 in Figure 6A), transcriptional induction of the mRNA

504    and protein of the stress gene by a transcription factor that is activated by the altered controlled

505    state (step 2), and lastly a global translational inhibition of proteins nonessential to the stress

506    response but necessary for cell functions (step 3). The model recapitulated the general pattern of

507    the dynamic and concentration-response of the transcriptome, proteome and phosphoproteome

508    observed in the present study. The transient spikes of the active phospho-stress protein (Ga) at

509    early timepoints which return to lower steady-state levels upon mild stress (Figure 6B) are

510    consistent with the temporal profile of the phosphoproteome observed in doxorubicin-treated

511    HepG2 cells (Figure 4B). Such dynamics are due to the initial perturbation by the stressor S and

512    subsequent engagement of the posttranslational feedback that brings the controlled state (Y) to

513    a nearly basal level. During this time frame of 6 hours, no transcription of mRNA (M) is tangibly

514    induced. Simulation of 24 hours exposure to the stressor resulted in concentration-response of

515    different sensitivity (Figure 6C). The active stress protein (Ga) exhibited a response that arises at

516    a low S level, while the M and total protein responses takes off at a much higher S level around

517    10. At this S level, the cell function protein (CFP) expression begins to be repressed with the

518    controlled state Y deviating from the baseline (Figure 6D), demarcating a PoD that may be linked

519    to apical endpoint changes.

520

521    **Discussion**

522    The transcriptome, proteome, and phosphoproteome of the cell have unique properties, with

523    information constantly flowing across these scales of biology. In the present study, we

524    demonstrated with coumarin and doxorubicin, two compounds with fundamentally distinct

525    molecular initiating events and modes of action, that phosphoproteomics changes occur not only

526    earlier in time as expected, but also at lower chemical concentrations, compared with proteomics

527    and transcriptomics alterations. As a result, changes in the phosphoproteome can provide

528    sensitive markers compared with changes in the proteome and transcriptome to indicate

529    alterations in cellular state following chemical exposure. Although only two compounds were

530    examined here, to our knowledge, this is the first study that compared multi-omics changes

531    across many concentrations and time points with replicates.

532    A single-omics technique such as in vitro high throughput transcriptomics has recently been

533    shown to be suitable for NAM-based hazard evaluation of environmental chemicals[69]. In

534    particular, high throughput transcriptomics has been used in lower tiers of NGRA assessments

535    as a conservative estimate of a quantitative POD in the 'protection not prediction paradigm' with

536    the aim of casting the broadest net possible for capturing the potential relevant bioactivity

537    associated with chemical treatment[70]. However, the use of a single omics techniques is unlikely

538    to lead to systematic understanding of pathways' response to chemical exposure and hence

539    elucidate on the mode of action of the substance. This is because a single-omics technique

540    measures biomolecule of a specific type, e.g. RNAs in case of transcriptomics, and thus captures

20

541    time-specific changes only for a small subset of components of a particular pathway. Therefore,

542    where residual uncertainty in a safety assessment means that such mechanistic understanding

543    is needed, other omics technologies may provide valuable data.

544       Proteomics techniques have developed rapidly over the past decade and are now being able

545    to identify and quantify several thousands of proteins from a single sample. Proteins represent

546    the biomolecules that directly operate in the cells and are therefore closer to the functional level.

547    Several studies have shown transcript expression levels for a specific transcript product may not

548    correlate to its protein expression level[71-74]. Indeed, besides the transcriptionally controlled

549    effects on protein abundance, there are translational and posttranslational effects that are not

550    reflected on the transcriptome level. There are many different types of PTMs but the most

551    abundant PTM is phosphorylation that has been the subject of this work. Sampadi et al has

552    recently demonstrated in a phosphoproteomics study that chemical stressors with different

553    modes of action can induce distinctive and complex phosphorylation signaling patterns[75]. In this

554    work we were able to detect another layer of biological response upon chemical exposure, by

555    identifying differentially expressed proteins and phosphosites.

556       In the era of NAM, a WoE approach that integrates multiple data streams is increasingly

557    adopted in the Next Generation Risk Assessement. Transcriptomics has gained tremendous

558    traction as an emerging high-coverage omics platform[76] and its importance to

559    mechanistically-based safety assessment should be better appreciated and interpreted.

560    Confidence in the use of transcriptomically-determined PoDs will increase if mechanistic

561    justifications can be provided in the larger context of cellular responses to chemical perturbations.

562    This is of particular importance in cases when NAMs used in lower tiers of risk assessment do

563    not provide sufficient information to make a decision on the absence of biological activity for a

564    given exposure scenario. In these cases, while transcriptionally-mediated cytoprotective gene

565    induction is well understood, other protective mechanisms that operate before transcriptional

566    induction is initiated are no less important biologically and can be exploited as biomarkers to

567    assess the degree of cellular perturbation. Here we compared changes across transcriptomic,

568     proteomic and phosphoproteomic measurements obtained with many replicates, concentration

569     and time points to understand the sensitivity of the three omics techniques in response to a

570     toxicant. We have demonstrated that phosphoproteomics changes occur not only earlier in time

571     as expected but also at low chemical concentrations and hence are proximal to the very early

572     effects induced by chemical treatment. Therefore, phosphoproteomics and proteomics changes

573     may play an essential role in investigating mechanisms of early adaptation and protection in cells.

574     Such non-transcriptomic omics data can be cross-referenced with and corroborate the

575     transcriptomically defined PoD as part of the multi-omics WoE approach.

576     Although far from being as sensitive as the phosphoproteome, the proteome exhibited

577     abundance changes of hundreds of proteins as early as 10 min in HepG2 cells after coumarin

578     treatment (Figure 3). Protein half-lives in mammalian cells are generally in the order of hours on

579     average, therefore at 10 min of exposure, little change would be expected in protein abundance.

580     However, proteins can differ in turnover rates dramatically, across several orders of magnitude[77],

581     and many of them are shorted-lived[53]. Protein stability is also highly regulated, many with

582     half-lives shorter than 20 min or even as short as a few minutes[78-81]. Therefore, if coumarin

583     treatment leads to altered protein synthesis or degradation, protein abundance changes can be

584     observed in 10 min for fast-turnover proteins.

585     The current analysis showed that integration of different omics layers to be used in toxicology

586     is not straightforward and indeed poses many challenges as recently reviewed[82]. One of the

587     challenges represents the choice of time points for different experiments. The choice of time

588     points used in this study has been based on the previous reports[8, 9], although we are aware that

589     this is a complex issue and there is not only a time variance between different omics layers, e.g.

590     proteome is downstream of the transcriptome, but also different biological processes occur on

591     different time scale within a single omics layer, e.g. translation occurs on a different time scale

592     from cell division. In addition, since proteomics and phosphoproteomics have not been routinely

593     used as NAM-based tool in hazard evaluation, their reproducibility of data acquisition and data

594     analysis demand more consideration. Furthermore, the coverage of expressed proteins,

595    phosphosites and transcripts needs to be addressed in order to ensure that relevant biology has

596    been sufficiently covered. Finally, the application of such a multi-omics approach to case studies

597    plays a critical role in building capability, understanding and ultimately confidence in bioactivity

598    characterization as integrating multi-omics is beginning to be considered in toxicity testing and

599    drug development[11, 12, 82, 83]. Detailed pathway analyses of the phosphoproteomics, proteomics,

600    and transcriptomics dataset reported in this study and derivation of associated PoDs at different

601    omics levels will be reported in separate upcoming publications to further reveal mechanistic

602    underpinnings for the tiered adaptive cellular response.

603    In summary, we propose to further evaluate the potential of multi-omics and its application in

604    Next Generation Risk Assessment in future using case study chemicals. We have presented

605    promising results by assessing proteomics and phosphoproteomics along with transcriptomics

606    and strongly believe that such integration of multiple omics data sets will offer a substantial

607    improvement in detecting molecular responses due to more complete representation of the

608    perturbed toxicity pathways.

609

610    **Acknowledgments**

622

**Disclosure statement**

624    No potential conflict of interest was reported by the authors.

**References**

( 1 ) Paul Friedman, K.; Gagne, M.; Loo, L.-H.; Karamertzanis, P.; Netzeva, T.; Sobanski, T.; Franzosa, J. A.; Richard, A. M.; Lougee, R. R.; Gissi, A.; Lee, J.-Y. J.; Angrish, M.; Dorne, J. L.; Foster, S.; Raffaele, K.; Bahadori, T.; Gwinn, M. R.; Lambert, J.; Whelan, M.; Rasenberg, M.; Barton-Maclaren, T.;Thomas, R. S. Utility of in vitro bioactivity as a lower bound estimate of in vivo adverse effect levels and in risk-based prioritization. *Toxicological Sciences.* **2019,** *173*, (1), 202-225.

( 2 ) Krewski, D.; Andersen, M. E.; Tyshenko, M. G.; Krishnan, K.; Hartung, T.; Boekelheide, K.; Wambaugh, J. F.; Jones, D.; Whelan, M.; Thomas, R.; Yauk, C.; Barton-Maclaren, T.;Cote, I. Toxicity testing in the 21st century: Progress in the past decade and future perspectives. *Archives of Toxicology.* **2020,** *94*, (1), 1-58.

( 3 ) Dent, M. P.; Vaillancourt, E.; Thomas, R. S.; Carmichael, P. L.; Ouedraogo, G.; Kojima, H.; Barroso, J.; Ansell, J.; Barton-Maclaren, T. S.; Bennekou, S. H.; Boekelheide, K.; Ezendam, J.; Field, J.; Fitzpatrick, S.; Hatao, M.; Kreiling, R.; Lorencini, M.; Mahony, C.; Montemayor, B.; Mazaro-Costa, R.; Oliveira, J.; Rogiers, V.; Smegal, D.; Taalman, R.; Tokura, Y.; Verma, R.; Willett, C.;Yang, C. Paving the way for application of next generation risk assessment to safety decision-making for cosmetic ingredients. *Regulatory Toxicology and Pharmacology.* **2021,** *125*, 105026.

( 4 )Simmons, S. O.; Fan, C. Y.;Ramabhadran, R. Cellular stress response pathway system as a sentinel ensemble in toxicological screening. *Toxicol Sci.* **2009,** *111*, (2), 202-25.

( 5 ) Zhang, Q.; Bhattacharya, S.; Pi, J.; Clewell, R. A.; Carmichael, P. L.;Andersen, M. E. Adaptive posttranslational control in cellular stress response pathways and its relationship to toxicity testing and safety assessment. *Toxicol Sci.* **2015,** *147*, (2), 302-16.

( 6 ) Bergamini, G.; Bell, K.; Shimamura, S.; Werner, T.; Cansfield, A.; Müller, K.; Perrin, J.; Rau, C.; Ellard, K.; Hopf, C.; Doce, C.; Leggate, D.; Mangano, R.; Mathieson, T.; O'Mahony, A.; Plavec, I.; Rharbaoui, F.; Reinhard, F.; Savitski, M. M.; Ramsden, N.; Hirsch, E.; Drewes, G.; Rausch, O.; Bantscheff, M.;Neubauer, G. A selective inhibitor reveals pi3kγ dependence of t(h)17 cell differentiation. *Nat Chem Biol.* **2012,** *8*, (6), 576-82.

( 7 ) Hendriks, G.; Derr, R. S.; Misovic, B.; Morolli, B.; Calléja, F. M.;Vrieling, H. The extended

654 toxtracker assay discriminates between induction of DNA damage, oxidative stress, and protein
655 misfolding. *Toxicol Sci.* **2016,** *150*, (1), 190-203.

656 ( 8 ) Yuan, H.; Zhang, Q.; Guo, J.; Zhang, T.; Zhao, J.; Li, J.; White, A.; Carmichael, P. L.;
657 Westmoreland, C.;Peng, S. A pgc-1α-mediated transcriptional network maintains mitochondrial
658 redox and bioenergetic homeostasis against doxorubicin-induced toxicity in human
659 cardiomyocytes: Implementation of tt21c. *Toxicol Sci.* **2016,** *150*, (2), 400-17.

660 ( 9 )Baltazar, M. T.; Cable, S.; Carmichael, P. L.; Cubberley, R.; Cull, T.; Delagrange, M.; Dent, M.
661 P.; Hatherell, S.; Houghton, J.; Kukic, P.; Li, H.; Lee, M. Y.; Malcomber, S.; Middleton, A. M.;
662 Moxon, T. E.; Nathanail, A. V.; Nicol, B.; Pendlington, R.; Reynolds, G.; Reynolds, J.; White,
663 A.;Westmoreland, C. A next-generation risk assessment case study for coumarin in cosmetic
664 products. *Toxicol. Sci.* **2020,** *176*, (1), 236-252.

665 ( 10 ) Thomas, R. S.; Bahadori, T.; Buckley, T. J.; Cowden, J.; Deisenroth, C.; Dionisio, K. L.;
666 Frithsen, J. B.; Grulke, C. M.; Gwinn, M. R.; Harrill, J. A.; Higuchi, M.; Houck, K. A.; Hughes, M. F.;
667 Hunter, E. S.; Isaacs, K. K.; Judson, R. S.; Knudsen, T. B.; Lambert, J. C.; Linnenbrink, M.; Martin,
668 T. M.; Newton, S. R.; Padilla, S.; Patlewicz, G.; Paul-Friedman, K.; Phillips, K. A.; Richard, A. M.;
669 Sams, R.; Shafer, T. J.; Setzer, R. W.; Shah, I.; Simmons, J. E.; Simmons, S. O.; Singh, A.;
670 Sobus, J. R.; Strynar, M.; Swank, A.; Tornero-Valez, R.; Ulrich, E. M.; Villeneuve, D. L.;
671 Wambaugh, J. F.; Wetmore, B. A.;Williams, A. J. The next generation blueprint of computational
672 toxicology at the u.S. Environmental protection agency. *Toxicol Sci.* **2019,** *169*, (2), 317-332.

673 ( 11 )Wilmes, A.; Bielow, C.; Ranninger, C.; Bellwon, P.; Aschauer, L.; Limonciel, A.; Chassaigne,
674 H.; Kristl, T.; Aiche, S.; Huber, C. G.; Guillou, C.; Hewitt, P.; Leonard, M. O.; Dekant, W.; Bois,
675 F.;Jennings, P. Mechanism of cisplatin proximal tubule toxicity revealed by integrating
676 transcriptomics, proteomics, metabolomics and biokinetics. *Toxicol In Vitro.* **2015,** *30*, (1 Pt A),
677 117-27.

678 ( 12 )Wilmes, A.; Limonciel, A.; Aschauer, L.; Moenks, K.; Bielow, C.; Leonard, M. O.; Hamon, J.;
679 Carpi, D.; Ruzek, S.; Handler, A.; Schmal, O.; Herrgen, K.; Bellwon, P.; Burek, C.; Truisi, G. L.;
680 Hewitt, P.; Di Consiglio, E.; Testai, E.; Blaauboer, B. J.; Guillou, C.; Huber, C. G.; Lukas, A.;
681 Pfaller, W.; Mueller, S. O.; Bois, F. Y.; Dekant, W.;Jennings, P. Application of integrated
682 transcriptomic, proteomic and metabolomic profiling for the delineation of mechanisms of drug
683 induced cell stress. *J Proteomics.* **2013,** *79*, 180-94.

684　( 13 ) Hudson, K. M.; Shiver, E.; Yu, J.; Mehta, S.; Jima, D. D.; Kane, M. A.; Patisaul, H.
685　B.;Cowley, M. Transcriptomic, proteomic, and metabolomic analyses identify candidate
686　pathways linking maternal cadmium exposure to altered neurodevelopment and behavior.
687　*Scientific Reports.* **2021,** *11*, (1), 16302.

688　( 14 ) Gatzidou, E. T.; Zira, A. N.;Theocharis, S. E. Toxicogenomics: A pivotal piece in the puzzle
689　of toxicological research. *J Appl Toxicol.* **2007,** *27*, (4), 302-9.

690　( 15 ) Van Hummelen, P.;Sasaki, J. State-of-the-art genomics approaches in toxicology. *Mutat*
691　*Res.* **2010,** *705*, (3), 165-71.

692　( 16 ) Chepelev, N. L.; Moffat, I. D.; Labib, S.; Bourdon-Lacombe, J.; Kuo, B.; Buick, J. K.;
693　Lemieux, F.; Malik, A. I.; Halappanavar, S.; Williams, A.;Yauk, C. L. Integrating toxicogenomics
694　into human health risk assessment: Lessons learned from the benzo[a]pyrene case study. *Crit.*
695　*Rev. Toxicol.* **2015,** *45*, (1), 44-52.

696　( 17 )Farmahin, R.; Williams, A.; Kuo, B.; Chepelev, N. L.; Thomas, R. S.; Barton-Maclaren, T. S.;
697　Curran, I. H.; Nong, A.; Wade, M. G.;Yauk, C. L. Recommended approaches in the application of
698　toxicogenomics to derive points of departure for chemical risk assessment. *Arch Toxicol.* **2017,**
699　*91*, (5), 2045-2065.

700　( 18 ) Thomas, R. S.; Wesselkamper, S. C.; Wang, N. C.; Zhao, Q. J.; Petersen, D. D.; Lambert,
701　J. C.; Cote, I.; Yang, L.; Healy, E.; Black, M. B.; Clewell, H. J., 3rd; Allen, B. C.;Andersen, M. E.
702　Temporal concordance between apical and transcriptional points of departure for chemical risk
703　assessment. *Toxicol. Sci.* **2013,** *134*, (1), 180-94.

704　( 19 )Moffat, I.; Chepelev, N.; Labib, S.; Bourdon-Lacombe, J.; Kuo, B.; Buick, J. K.; Lemieux, F.;
705　Williams, A.; Halappanavar, S.; Malik, A.; Luijten, M.; Aubrecht, J.; Hyduke, D. R.; Fornace, A. J.,
706　Jr.; Swartz, C. D.; Recio, L.;Yauk, C. L. Comparison of toxicogenomics and traditional
707　approaches to inform mode of action and points of departure in human health risk assessment of
708　benzo[a]pyrene in drinking water. *Crit. Rev. Toxicol.* **2015,** *45*, (1), 1-43.

709　( 20 )Zhou, Y. H.; Cichocki, J. A.; Soldatow, V. Y.; Scholl, E. H.; Gallins, P. J.; Jima, D.; Yoo, H. S.;
710　Chiu, W. A.; Wright, F. A.;Rusyn, I. Comparative dose-response analysis of liver and kidney

711 transcriptomic effects of trichloroethylene and tetrachloroethylene in b6c3f1 mouse. *Toxicol Sci.*
712 **2017,** *160*, (1), 95-110.

713 ( 21 ) Dean, J. L.; Zhao, Q. J.; Lambert, J. C.; Hawkins, B. S.; Thomas, R. S.;Wesselkamper, S.
714 C. Application of gene set enrichment analysis for identification of chemically induced,
715 biologically relevant transcriptomic networks and potential utilization in human health risk
716 assessment. *Toxicol Sci.* **2017,** *157*, (1), 85-99.

717 ( 22 ) Bhat, V. S.; Hester, S. D.; Nesnow, S.;Eastmond, D. A. Concordance of transcriptional and
718 apical benchmark dose levels for conazole-induced liver effects in mice. *Toxicol Sci.* **2013,** *136*,
719 (1), 205-15.

720 ( 23 )Harrill, J. A.; Everett, L. J.; Haggard, D. E.; Sheffield, T.; Bundy, J. L.; Willis, C. M.; Thomas,
721 R. S.; Shah, I.;Judson, R. S. High-throughput transcriptomics platform for screening
722 environmental chemicals. *Toxicological Sciences.* **2021,** *181*, (1), 68-89.

723 ( 24 ) Yang, L.; Allen, B. C.;Thomas, R. S. Bmdexpress: A software tool for the benchmark dose
724 analyses of genomic data. *BMC genomics.* **2007,** *8*, (1), 1-8.

725 ( 25 ) Phillips, J. R.; Svoboda, D. L.; Tandon, A.; Patel, S.; Sedykh, A.; Mav, D.; Kuo, B.; Yauk, C.
726 L.; Yang, L.; Thomas, R. S.; Gift, J. S.; Davis, J. A.; Olszyk, L.; Merrick, B. A.; Paules, R. S.;
727 Parham, F.; Saddler, T.; Shah, R. R.;Auerbach, S. S. Bmdexpress 2: Enhanced transcriptomic
728 dose-response analysis workflow. *Bioinformatics.* **2019,** *35*, (10), 1780-1782.

729 ( 26 ) Buttgereit, F.;Brand, M. D. A hierarchy of atp-consuming processes in mammalian cells.
730 *Biochem J.* **1995,** *312 ( Pt 1)*, 163-7.

731 ( 27 ) Hoffmann, F.;Rinas, U. On-line estimation of the metabolic burden resulting from the
732 synthesis of plasmid-encoded and heat-shock proteins by monitoring respiratory energy
733 generation. *Biotechnol. Bioeng.* **2001,** *76*, (4), 333-40.

734 ( 28 )Klaassen, C. D.;Liu, J. Induction of metallothionein as an adaptive mechanism affecting the
735 magnitude and progression of toxicological injury. *Environ Health Perspect.* **1998,** *106 Suppl 1*,
736 297-300.

737 ( 29 ) Pi, J.; Zhang, Q.; Woods, C. G.; Wong, V.; Collins, S.;Andersen, M. E. Activation of

738 nrf2-mediated oxidative stress response in macrophages by hypochlorous acid. *Toxicol Appl*

739 *Pharmacol.* **2008,** *226*, (3), 236-43.

740 ( 30 ) Sokolova, I. M. Energy-limited tolerance to stress as a conceptual framework to integrate

741 the effects of multiple stressors. *Integr Comp Biol.* **2013,** *53*, (4), 597-608.

742 ( 31 ) Chadwick, J. G., Jr.; Nislow, K. H.;McCormick, S. D. Thermal onset of cellular and

743 endocrine stress responses correspond to ecological limits in brook trout, an iconic cold-water

744 fish. *Conserv Physiol.* **2015,** *3*, (1), cov017.

745 ( 32 ) Zhang, Q.; Li, J.; Middleton, A.; Bhattacharya, S.;Conolly, R. B. Bridging the data gap from

746 in vitro toxicity testing to chemical safety assessment through computational modeling. *Frontiers*

747 *in Public Health.* **2018,** *6*, (261).

748 ( 33 ) Mendes, C.;Serpa, J. Metabolic remodelling: An accomplice for new therapeutic strategies

749 to fight lung cancer. *Antioxidants (Basel).* **2019,** *8*, (12).

750 ( 34 ) Rein, T. Post-translational modifications and stress adaptation: The paradigm of fkbp51.

751 *Biochem Soc Trans.* **2020,** *48*, (2), 441-449.

752 ( 35 ) Gitan, R. S.;Eide, D. J. Zinc-regulated ubiquitin conjugation signals endocytosis of the

753 yeast zrt1 zinc transporter. *Biochem J.* **2000,** *346 Pt 2*, 329-36.

754 ( 36 ) Dihazi, H.; Kessler, R.;Eschrich, K. High osmolarity glycerol (hog) pathway-induced

755 phosphorylation and activation of 6-phosphofructo-2-kinase are essential for glycerol

756 accumulation and yeast cell proliferation under hyperosmotic stress. *J. Biol. Chem.* **2004,** *279*,

757 (23), 23961-8.

758 ( 37 )Krejsa, C. M.; Franklin, C. C.; White, C. C.; Ledbetter, J. A.; Schieven, G. L.;Kavanagh, T. J.

759 Rapid activation of glutamate cysteine ligase following oxidative stress. *J. Biol. Chem.* **2010,** *285*,

760 (21), 16116-24.

761    ( 38 ) Zhao, M.; Wu, F.;Xu, P. Development of a rapid high-efficiency scalable process for

762    acetylated sus scrofa cationic trypsin production from escherichia coli inclusion bodies. *Protein*

763    *expression and purification.* **2015,** *116*.

764    ( 39 ) Hatherell, S.; Baltazar, M. T.; Reynolds, J.; Carmichael, P. L.; Dent, M.; Li, H.; Ryder, S.;

765    White, A.; Walker, P.;Middleton, A. M. Identifying and characterizing stress pathways of concern

766    for consumer safety in next-generation risk assessment. *Toxicological Sciences.* **2020,** *176*, (1),

767    11-33.

768    ( 40 ) Li, Y.; Dammer, E. B.; Gao, Y.; Lan, Q.; Villamil, M. A.; Duong, D. M.; Zhang, C.; Ping, L.;

769    Lauinger, L.; Flick, K.; Xu, Z.; Wei, W.; Xing, X.; Chang, L.; Jin, J.; Hong, X.; Zhu, Y.; Wu, J.; Deng,

770    Z.; He, F.; Kaiser, P.;Xu, P. Proteomics links ubiquitin chain topology change to transcription

771    factor activation. *Mol. Cell.* **2019,** *76*, (1), 126-137.e7.

772    ( 41 ) Pertea, M.; Kim, D.; Pertea, G. M.; Leek, J. T.;Salzberg, S. L. Transcript-level expression

773    analysis of rna-seq experiments with hisat, stringtie and ballgown. *Nature protocols.* **2016,** *11*, (9),

774    1650-67.

775    ( 42 ) Xu, P.; Duong, D. M.;Peng, J. Systematical optimization of reverse-phase chromatography

776    for shotgun proteomics. *Journal of proteome research.* **2009,** *8*, (8), 3944-50.

777    ( 43 ) Wu, F.; Zhao, M.; Zhang, Y.; Su, N.; Xiong, Z.;Xu, P. Recombinant acetylated trypsin

778    demonstrates superior stability and higher activity than commercial products in quantitative

779    proteomics studies. *Rapid communications in mass spectrometry : RCM.* **2016,** *30*, (8), 1059-66.

780    ( 44 ) Peng, X.; Xu, F.; Liu, S.; Li, S.; Huang, Q.; Chang, L.; Wang, L.; Ma, X.; He, F.;Xu, P.

781    Identification of missing proteins in the phosphoproteome of kidney cancer. *Journal of proteome*

782    *research.* **2017,** *16*, (12), 4364-4373.

783    ( 45 ) Xu, F.; Yu, L.; Peng, X.; Zhang, J.; Li, S.; Liu, S.; Yin, Y.; An, Z.; Wang, F.; Fu, Y.;Xu, P.

784    Unambiguous phosphosite localization through the combination of trypsin and lysarginase mirror

785    spectra in a large-scale phosphoproteome study. *Journal of proteome research.* **2020,** *19*, (6),

786    2185-2194.

787   ( 46 )Zhai, L.; Chang, C.; Li, N.; Duong, D. M.; Chen, H.; Deng, Z.; Yang, J.; Hong, X.; Zhu, Y.;Xu,

788   P. Systematic research on the pretreatment of peptides for quantitative proteomics using a c□□
789   microcolumn. *Proteomics.* **2013,** *13*, (15), 2229-37.

790   ( 47 ) Tyanova, S.; Temu, T.; Sinitcyn, P.; Carlson, A.; Hein, M. Y.; Geiger, T.; Mann, M.;Cox, J.

791   The perseus computational platform for comprehensive analysis of (prote)omics data. *Nature*
792   *methods.* **2016**.

793   ( 48 ) Wickham, H. *Ggplot2: Elegant graphics for data analysis.* Springer Publishing Company,

794   Incorporated: 2009.

795   ( 49 ) Team, R. C. R: A language and environment for statistical computing. **2013**.

796   ( 50 )Romanov, S.; Medvedev, A.; Gambarian, M.; Poltoratskaya, N.; Moeser, M.; Medvedeva, L.;

797   Gambarian, M.; Diatchenko, L.;Makarov, S. Homogeneous reporter system enables quantitative
798   functional assessment of multiple transcription factors. *Nature methods.* **2008,** *5*, (3), 253-60.

799   ( 51 )Martin, M. T.; Dix, D. J.; Judson, R. S.; Kavlock, R. J.; Reif, D. M.; Richard, A. M.; Rotroff, D.

800   M.; Romanov, S.; Medvedev, A.; Poltoratskaya, N.; Gambarian, M.; Moeser, M.; Makarov, S.
801   S.;Houck, K. A. Impact of environmental chemicals on key transcription regulators and
802   correlation to toxicity end points within epa's toxcast program. *Chemical Research in Toxicology.*
803   **2010,** *23*, (3), 578-590.

804   ( 52 ) Giuliano, K. A.; Gough, A. H.; Taylor, D. L.; Vernetti, L. A.;Johnston, P. A. Early safety

805   assessment using cellular systems biology yields insights into mechanisms of action. *Journal of*
806   *biomolecular screening.* **2010,** *15*, (7), 783-97.

807   ( 53 ) Li, J.; Cai, Z.; Vaites, L. P.; Shen, N.; Mitchell, D. C.; Huttlin, E. L.; Paulo, J. A.; Harry, B.

808   L.;Gygi, S. P. Proteome-wide mapping of short-lived proteins in human cells. *Molecular Cell.*
809   **2021,** *81*, (22), 4722-4735.e5.

810   ( 54 ) Hatherell, S.; Baltazar, M. T.; Reynolds, J.; Carmichael, P. L.; Dent, M.; Li, H.; Ryder, S.;

811   White, A.; Walker, P.;Middleton, A. M. Identifying and characterizing stress pathways of concern

812   for consumer safety in next-generation risk assessment. *Toxicol. Sci.* **2020,** *176*, (1), 11-33.

813   ( 55 ) Lenaz, L.;Page, J. A. Cardiotoxicity of adriamycin and related anthracyclines. *Cancer*
814   *Treatment Reviews.* **1976,** *3*, (3), 111-120.

815   ( 56 ) Yuan, H.; Zhang, Q.; Guo, J.; Zhang, T.; Zhao, J.; Li, J.; White, A.; Carmichael, P. L.;
816   Westmoreland, C.;Peng, S. A pgc-1α-mediated transcriptional network maintains mitochondrial
817   redox and bioenergetic homeostasis against doxorubicin-induced toxicity in human
818   cardiomyocytes: Implementation of tt21c. *Toxicological Sciences.* **2016,** *150*, (2), 400-417.

819   ( 57 ) Chaudhari, U.; Nemade, H.; Wagh, V.; Gaspar, J. A.; Ellis, J. K.; Srinivasan, S. P.;
820   Spitkovski, D.; Nguemo, F.; Louisse, J.; Bremer, S.; Hescheler, J.; Keun, H. C.; Hengstler, J.
821   G.;Sachinidis, A. Identification of genomic biomarkers for anthracycline-induced cardiotoxicity in
822   human ipsc-derived cardiomyocytes: An in vitro repeated exposure toxicity approach for safety
823   assessment. *Archives of Toxicology.* **2016,** *90*, (11), 2763-2777.

824   ( 58 ) Bergström Lind, S.; Molin, M.; Savitski, M. M.; Emilsson, L.; Aström, J.; Hedberg, L.;
825   Adams, C.; Nielsen, M. L.; Engström, A.; Elfineh, L.; Andersson, E.; Zubarev, R. A.;Pettersson, U.
826   Immunoaffinity enrichments followed by mass spectrometric detection for studying global protein
827   tyrosine phosphorylation. *J. Proteome Res.* **2008,** *7*, (7), 2897-910.

828   ( 59 ) Bian, Y.; Li, L.; Dong, M.; Liu, X.; Kaneko, T.; Cheng, K.; Liu, H.; Voss, C.; Cao, X.; Wang,
829   Y.; Litchfield, D.; Ye, M.; Li, S. S.;Zou, H. Ultra-deep tyrosine phosphoproteomics enabled by a
830   phosphotyrosine superbinder. *Nat. Chem. Biol.* **2016,** *12*, (11), 959-966.

831   ( 60 ) Jassal, B.; Matthews, L.; Viteri, G.; Gong, C.; Lorente, P.; Fabregat, A.; Sidiropoulos, K.;
832   Cook, J.; Gillespie, M.; Haw, R.; Loney, F.; May, B.; Milacic, M.; Rothfels, K.; Sevilla, C.;
833   Shamovsky, V.; Shorser, S.; Varusai, T.; Weiser, J.; Wu, G.; Stein, L.; Hermjakob, H.;D'Eustachio,
834   P. The reactome pathway knowledgebase. *Nucleic Acids Res.* **2020,** *48*, (D1), D498-D503.

835   ( 61 ) Kim, H. S.; Lee, Y. S.;Kim, D. K. Doxorubicin exerts cytotoxic effects through cell cycle
836   arrest and fas-mediated cell death. *Pharmacology.* **2009,** *84*, (5), 300-309.

837   ( 62 )Hultman, I.; Haeggblom, L.; Rognmo, I.; Jansson Edqvist, J.; Blomberg, E.; Ali, R.; Phillips,

838  L.; Sandstedt, B.; Kogner, P.; Shirazi Fard, S.;Ährlund-Richter, L. Doxorubicin-provoked increase
839  of mitotic activity and concomitant drain of g0-pool in therapy-resistant be(2)-c neuroblastoma.
840  *PLOS ONE.* **2018,** *13*, (1), e0190970.

841  （63）Kobayashi, A.; Kang, M. I.; Watai, Y.; Tong, K. I.; Shibata, T.; Uchida, K.;Yamamoto, M.
842  Oxidative and electrophilic stresses activate nrf2 through inhibition of ubiquitination activity of
843  keap1. *Molecular and cellular biology.* **2006,** *26*, (1), 221-9.

844  （64）Kwak, M. K.; Itoh, K.; Yamamoto, M.;Kensler, T. W. Enhanced expression of the
845  transcription factor nrf2 by cancer chemopreventive agents: Role of antioxidant response
846  element-like sequences in the nrf2 promoter. *Molecular and cellular biology.* **2002,** *22*, (9),
847  2883-92.

848  （65）Feng, Z.; Zhang, H.; Levine, A. J.;Jin, S. The coordinate regulation of the p53 and mtor
849  pathways in cells. *Proceedings of the National Academy of Sciences of the United States of
850  America.* **2005,** *102*, (23), 8204-8209.

851  （66）Li, D. L.; Wang, Z. V.; Ding, G.; Tan, W.; Luo, X.; Criollo, A.; Xie, M.; Jiang, N.; May, H.;
852  Kyrychenko, V.; Schneider, J. W.; Gillette, T. G.;Hill, J. A. Doxorubicin blocks cardiomyocyte
853  autophagic flux by inhibiting lysosome acidification. *Circulation.* **2016,** *133*, (17), 1668-87.

854  （67）Li, R.; Huang, Y.; Semple, I.; Kim, M.; Zhang, Z.;Lee, J. H. Cardioprotective roles of sestrin
855  1 and sestrin 2 against doxorubicin cardiotoxicity. *Am J Physiol Heart Circ Physiol.* **2019,** *317*, (1),
856  H39-H48.

857  （68）Linares, J. F.; Amanchy, R.; Greis, K.; Diaz-Meco, M. T.;Moscat, J. Phosphorylation of p62
858  by cdk1 controls the timely transit of cells through mitosis and tumor cell proliferation. *Molecular
859  and cellular biology.* **2011,** *31*, (1), 105-17.

860  （69）Auerbach, S. S.;Paules, R. S. Genomic dose response: Successes, challenges, and next
861  steps. *Current Opinion in Toxicology.* **2018,** *11-12*, 84-92.

862  （70）Harrill, J.; Shah, I.; Setzer, R. W.; Haggard, D.; Auerbach, S.; Judson, R.;Thomas, R. S.
863  Considerations for strategic use of high-throughput transcriptomics chemical screening data in

864    regulatory decisions. *Curr Opin Toxicol.* **2019,** *15*, 64-75.

865    ( 71 ) Grün, D.; Kirchner, M.; Thierfelder, N.; Stoeckius, M.; Selbach, M.;Rajewsky, N.
866    Conservation of mrna and protein expression during development of c. elegans. *Cell Reports.*
867    **2014,** *6*, (3), 565-577.

868    ( 72 ) Maier, T.; Güell, M.;Serrano, L. Correlation of mrna and protein in complex biological
869    samples. *FEBS Lett.* **2009,** *583*, (24), 3966-73.

870    ( 73 ) Gygi, S. P.; Rochon, Y.; Franza, B. R.;Aebersold, R. Correlation between protein and mrna
871    abundance in yeast. *Mol Cell Biol.* **1999,** *19*, (3), 1720-30.

872    ( 74 ) Futcher, B.; Latter, G. I.; Monardo, P.; McLaughlin, C. S.;Garrels, J. I. A sampling of the
873    yeast proteome. *Mol Cell Biol.* **1999,** *19*, (11), 7357-68.

874    ( 75 )Sampadi, B.; Pines, A.; Munk, S.; Mišovic, B.; de Groot, A. J.; van de Water, B.; Olsen, J. V.;
875    Mullenders, L. H. F.;Vrieling, H. Quantitative phosphoproteomics to unravel the cellular response
876    to chemical stressors with different modes of action. *Arch. Toxicol.* **2020,** *94*, (5), 1655-1671.

877    ( 76 )Harrill, J. A.; Viant, M. R.; Yauk, C. L.; Sachana, M.; Gant, T. W.; Auerbach, S. S.; Beger, R.
878    D.; Bouhifd, M.; O'Brien, J.; Burgoon, L.; Caiment, F.; Carpi, D.; Chen, T.; Chorley, B. N.;
879    Colbourne, J.; Corvi, R.; Debrauwer, L.; O'Donovan, C.; Ebbels, T. M. D.; Ekman, D. R.;
880    Faulhammer, F.; Gribaldo, L.; Hilton, G. M.; Jones, S. P.; Kende, A.; Lawson, T. N.; Leite, S. B.;
881    Leonards, P. E. G.; Luijten, M.; Martin, A.; Moussa, L.; Rudaz, S.; Schmitz, O.; Sobanski, T.;
882    Strauss, V.; Vaccari, M.; Vijay, V.; Weber, R. J. M.; Williams, A. J.; Williams, A.; Thomas, R.
883    S.;Whelan, M. Progress towards an oecd reporting framework for transcriptomics and
884    metabolomics in regulatory toxicology. *Regulatory Toxicology and Pharmacology.* **2021,** *125*,
885    105020.

886    ( 77 ) Schwanhäusser, B.; Busse, D.; Li, N.; Dittmar, G.; Schuchhardt, J.; Wolf, J.; Chen,
887    W.;Selbach, M. Corrigendum: Global quantification of mammalian gene expression control.
888    *Nature.* **2013,** *495*, (7439), 126-7.

889    ( 78 ) Berra, E.; Roux, D.; Richard, D. E.;Pouysségur, J. Hypoxia-inducible factor-1 alpha (hif-1

890 alpha) escapes o(2)-driven proteasomal degradation irrespective of its subcellular localization:
891 Nucleus or cytoplasm. *EMBO Rep.* **2001,** *2*, (7), 615-20.

892 ( 79 ) Khalil, H. S.; Goltsov, A.; Langdon, S. P.; Harrison, D. J.; Bown, J.;Deeni, Y. Quantitative
893 analysis of nrf2 pathway reveals key elements of the regulatory circuits underlying antioxidant
894 response and proliferation of ovarian cancer cells. *J Biotechnol.* **2015,** *202*, 12-30.

895 ( 80 ) Heinzel, S.; Binh Giang, T.; Kan, A.; Marchingo, J. M.; Lye, B. K.; Corcoran, L. M.;Hodgkin,
896 P. D. A myc-dependent division timer complements a cell-death timer to regulate t cell and b cell
897 responses. *Nat Immunol.* **2017,** *18*, (1), 96-103.

898 ( 81 ) Levine, A. J. Targeting therapies for the p53 protein in cancer treatments. *Annual Review*
899 *of Cancer Biology.* **2019,** *3*, (1), 21-34.

900 ( 82 )Canzler, S.; Schor, J.; Busch, W.; Schubert, K.; Rolle-Kampczyk, U. E.; Seitz, H.; Kamp, H.;
901 von Bergen, M.; Buesen, R.;Hackermüller, J. Prospects and challenges of multi-omics data
902 integration in toxicology. *Arch Toxicol.* **2020,** *94*, (2), 371-388.

903 ( 83 ) Selevsek, N.; Caiment, F.; Nudischer, R.; Gmuender, H.; Agarkova, I.; Atkinson, F. L.;
904 Bachmann, I.; Baier, V.; Barel, G.; Bauer, C.; Boerno, S.; Bosc, N.; Clayton, O.; Cordes, H.; Deeb,
905 S.; Gotta, S.; Guye, P.; Hersey, A.; Hunter, F. M. I.; Kunz, L.; Lewalle, A.; Lienhard, M.; Merken, J.;
906 Minguet, J.; Oliveira, B.; Pluess, C.; Sarkans, U.; Schrooders, Y.; Schuchhardt, J.; Smit, I.; Thiel,
907 C.; Timmermann, B.; Verheijen, M.; Wittenberger, T.; Wolski, W.; Zerck, A.; Heymans, S.; Kuepfer,
908 L.; Roth, A.; Schlapbach, R.; Niederer, S.; Herwig, R.;Kleinjans, J. Network integration and
909 modelling of dynamic drug responses at multi-omics levels. *Communications Biology.* **2020,** *3*,
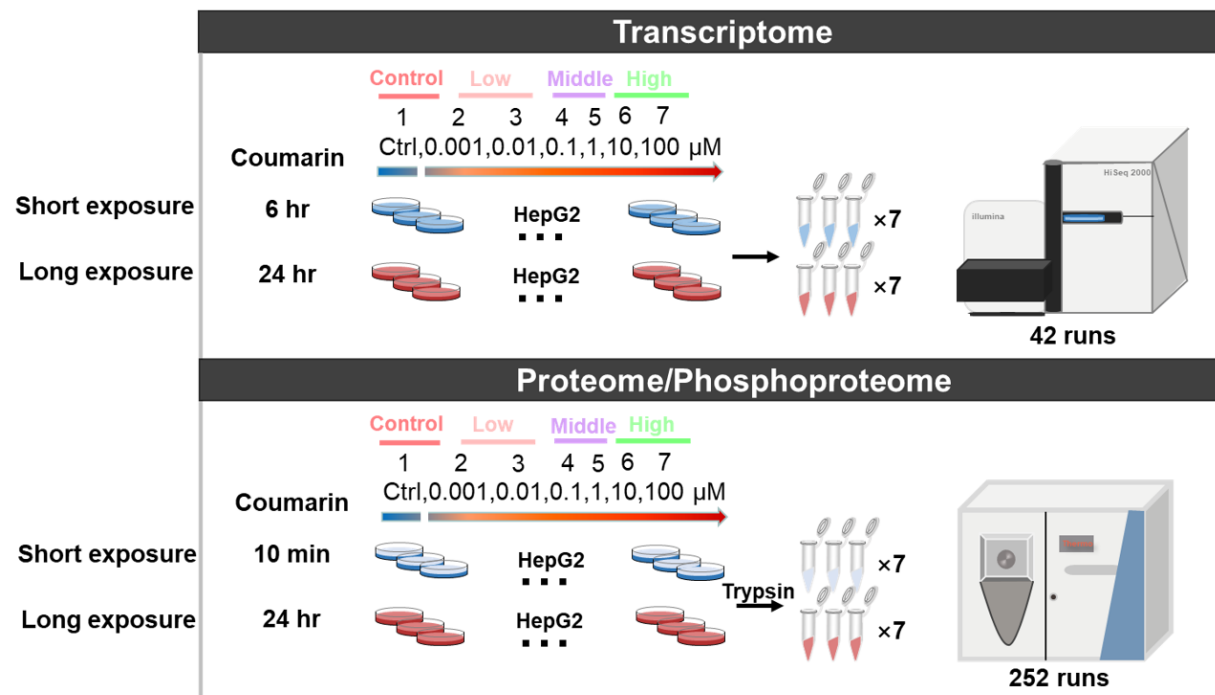910 (1), 573.

911

912

913 **Figures**

914

**Figure 1. The experimental procedures for multi-omics measurements of cellular response to coumarin.** The workflow of omics study for cellular response of coumarin treated HepG2 cells. In the transcriptomics study, in addition to vehicle control, HepG2 cells were treated with 6 concentrations of coumarin ranging from 0.001 to 100 μM as indicated. The concentrations are numerically coded as 1-7 as indicated for ease of referencing in other figures. The cells were recovered for RNAseq after treated for 6 and 24 hours, which were denoted as short-exposure and long-exposure, respectively. Each concentration-time experimental condition was repeated for three biological replicates. A total of 42 samples were collected for RNA-seq. In proteomics and phosphoproteomics studies all experimental conditions remained the same except that the treatment durations are 10 min and 6 hours.

925
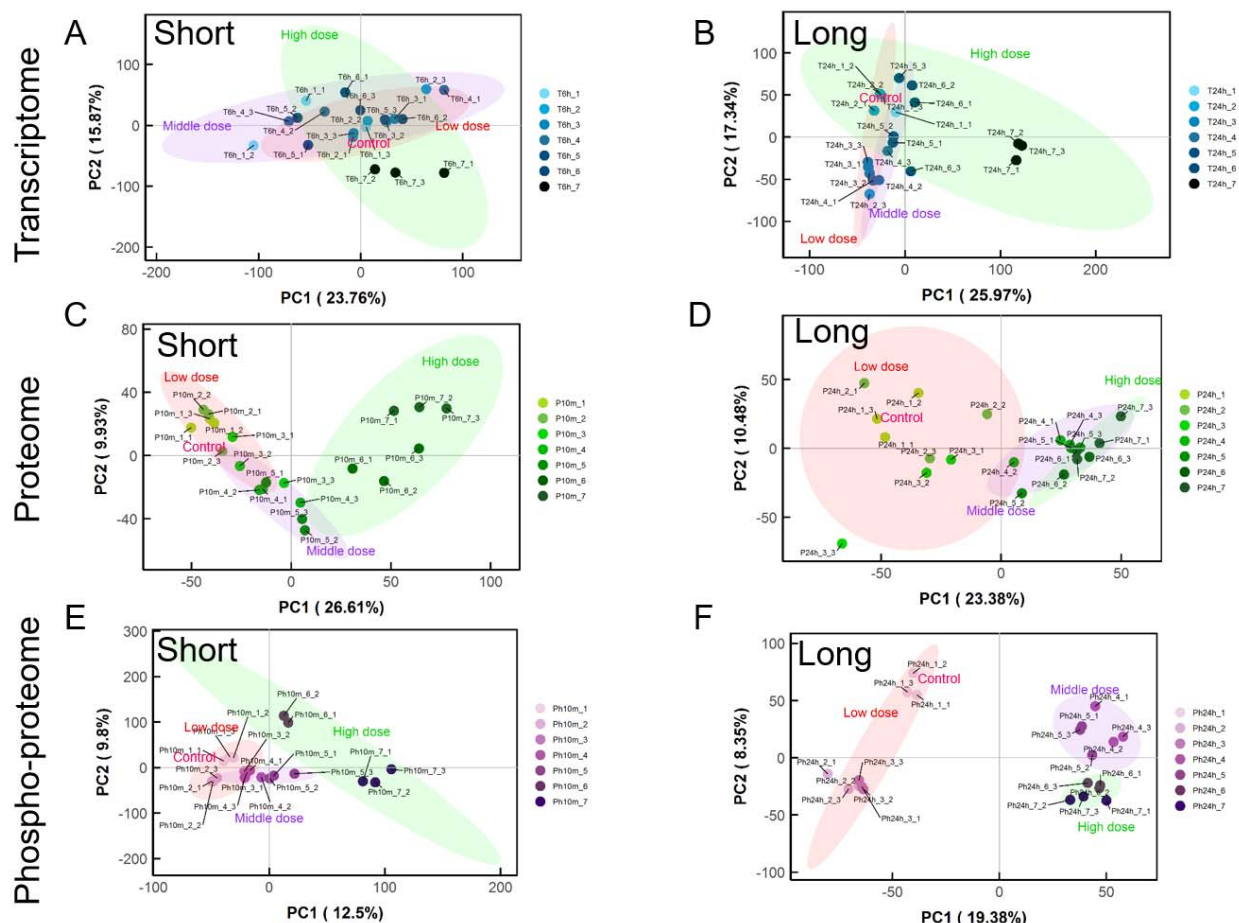
**Figure 2. PCA analysis of omics data generated from HepG2 cells treated with various concentrations of coumarin.**

(A & B) PCA analysis of transcriptomics data for short (6-hr) and long (24-hr) exposure to coumarin, respectively. (C & D) PCA analysis of proteomics data for short (10-min) and long (24-hr) exposure to coumarin, respectively. (E & F) PCA analysis of phosphoproteomics data for short (10 min) and long (24 hours) exposure to coumarin, respectively. Color-shaded ellipses encircle different coumarin dose groups: red, control group and low-dose (0-0.01 μM); pink, middle-dose (0.1-1 μM); and green, high-dose (10-100 μM).

A  The number of differentinal expressed gene/protein/phosphosite in HepG2 cell treated with coumarin

| Sample comparsion | Short exposure | | | Long exposure | | |
|---|---|---|---|---|---|---|
| | mRNA | Protein | Phosphosite | mRNA | Protein | Phosphosite |
| 0.001 VS Control | 10 | 186 | 1635 | 13 | 146 | 2341 |
| 0.01 VS Control | 8 | 188 | 1544 | 21 | 345 | 2126 |
| 0.1 VS Control | 9 | 419 | 2036 | 21 | 673 | 3331 |
| 1 VS Control | 12 | 376 | 1895 | 19 | 673 | 2944 |
| 10 VS Control | 22 | 625 | 2689 | 25 | 722 | 3567 |
| 100 VS Control | 78 | 729 | 3171 | 263 | 760 | 3568 |
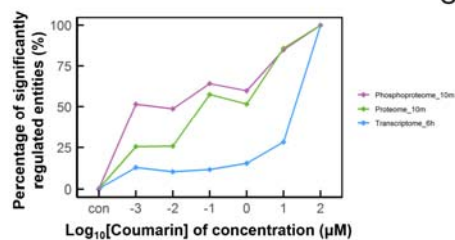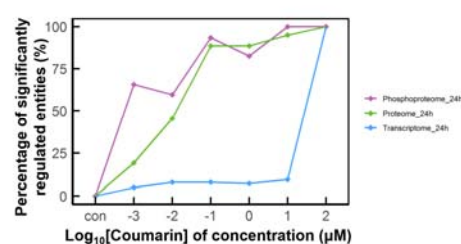
**Figure 3. Phosphoproteome is the most sensitive omics marker to detect cellular responses to low concentrations of coumarin in HepG2 cells.**

(A) The number of differentially altered features relative to control in the transcriptome, proteome and phosphoproteome of HepG2 cells treated with coumarin of various concentrations for short (10-30 min) or long durations (24 hours). (B & C) Percentage of differentially altered features normalized to the number of differentially altered features at the highest concentration (100 µM) for short (B) and long (C) exposures, respectively.
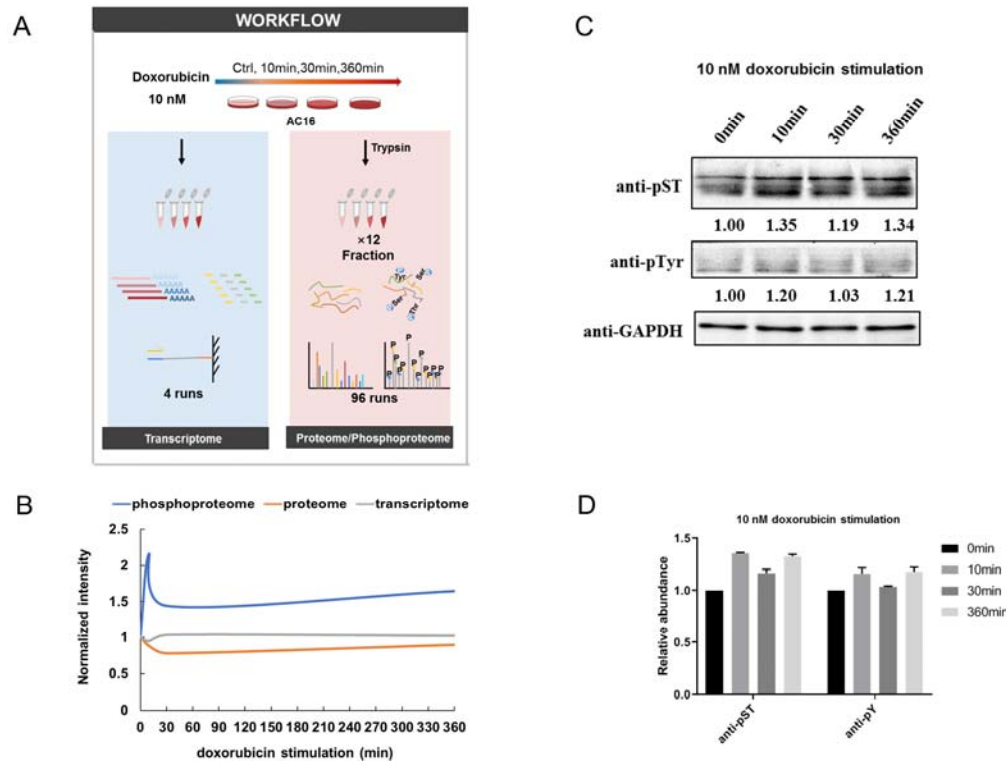
38

947

**Figure 4. Phosphoproteome is the most sensitive omics marker to detect cellular responses to doxorubicin at a low concentration in AC16 cells.**

(A) The workflow of omics study for cellular response of AC16 cells to 10 nM doxorubicin treatment for 0, 10, 30 and 360 min. A total of 4 samples were collected for RNA sequencing. For proteomics and phosphoproteomics, each of the sample had 12 fractions. (B) The relative intensity of abundance normalized to control at 0 min for transcriptome, proteome and phosphoproteome. (C) Western blot analysis of phospho-protein in total cell lysates extracted from AC16 cells treated with 10 nM doxorubicin for 10, 30, and 360 min. Anti-pST and anti-pTyr: pan antibodies used to detect phosphorylated serine/threonine and tyrosine respectively. (D) Quantification of (C).
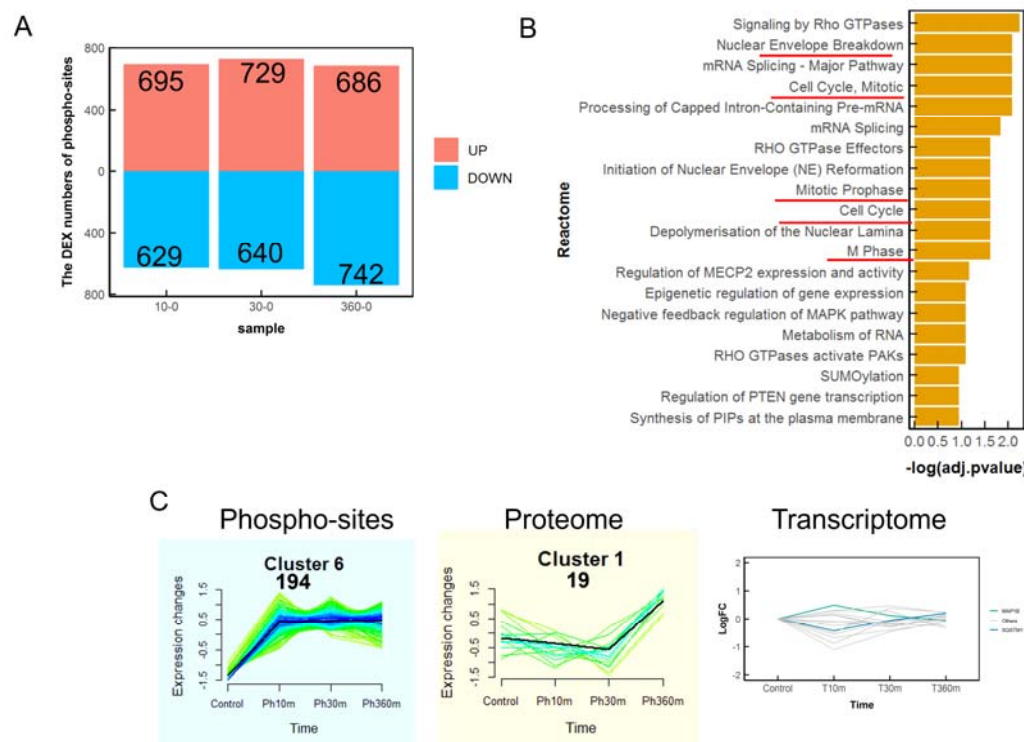
958

**Figure 5. Phosphoproteomics revealed sensitive pathway enrichment in low-concentration doxorubicin-treated AC16 cells.**

(A) The number of significantly up- and down-regulated phosphosites in AC16 cells treated with 10 nM doxorubicin for 10, 30, and 360 min (with FC > 2 or < 0.5). (B) GSEA-based enrichment analysis of GO biological processes up-regulated by10 nM doxorubicin treatment. All of the up-regulated phosphoproteins were combined for this analysis and top 20 Reactome pathways were displayed. (C) A total of 194 phosphosites were upregulated persistently throughout the 360-min duration of doxorubicin treatment. 19 proteins identified in the proteomics study form a cluster that exhibited upregulation only at 360 min. No significant changes in transcriptome were identified among the corresponding genes.
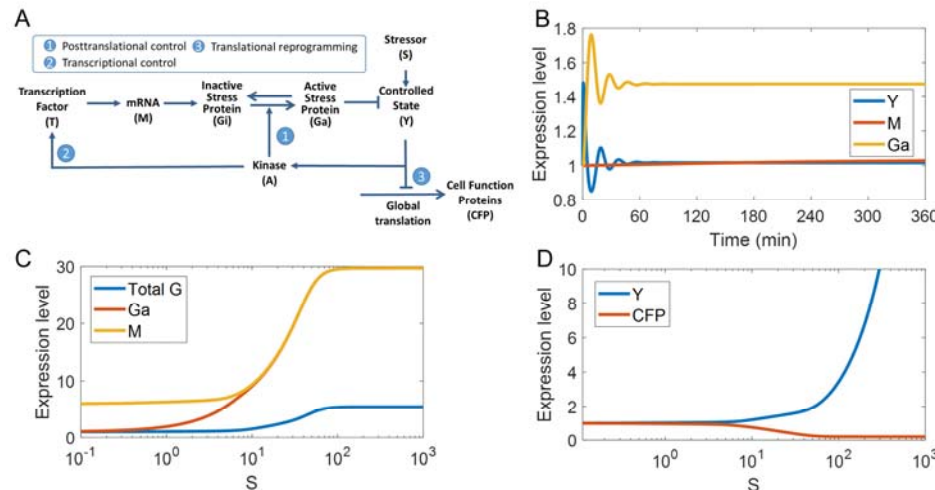
969



**Figure 6. Simulations of cell stress response by two-tiered transcriptional and posttranslational control.**

(A) Mode of cellular stress response to stressor S may involve both transcriptional and posttranslational control of the cellular state (Y). The transcriptional induction of mRNA (M) for stress gene (G) is activated by transcription factor (T) through pathway #2. Posttranslational modification control bypasses the slow-acting transcriptional loop by regulating the activities of preexisting inactive stress proteins (Gi) through phosphorylation to convert Gi into active stress protein (Ga) via pathway #1. The stress can also directly affect specialized cell function proteins (CFP) through step #3. Pointed arrows denote activation and blunted arrows denote inhibition. (B) Temporal responses of Y, Ga and M in response to a mild S level (0.5). (C) Dose responses of M, Ga and total G after 24-h exposure. (D) Dose responses of Y and CFP after 24-h exposure.



**Supplemental Figures**

Figure S1. Quality control for the transcriptomics study in HepG2 cells treated with Coumarin.

Figure S2. Quality control for the proteomics study in HepG2 cells treated with Coumarin.

Figure S3. Quality control for the phospho-proteomics study in HepG2 cells treated with Coumarin.

988 Figure S4. Pair-wise Pearson correlation analysis of phosphoproteomics, proteomics, and

989 transcriptomics samples of HepG2 cells treated with Coumarin.

990 Figure S5. Hierarchical clustering of the transcriptome, proteome, and phosphoproteome of

991 HepG2 cells treated with Coumarin.

992 Figure S6. Volcano plots of differentially expressed features in the proteome, phosphoproteome,

993 and transcriptome of HepG2 cells treated with Coumarin.

994 Figure S7.  Quality control for the transcriptomics study in AC16 cells treated with 10 nM

995 doxorubicin for 10, 30, and 360 min.

996 Figure S8. Quality control for the proteomics study in AC16 cells treated with 10 nM doxorubicin

997 for 10, 30, and 360 min.

998 Figure S9. Quality control for the phosphor-proteomics study in AC16 cells treated with 10 nM

999 doxorubicin for 10, 30, and 360 min.

1000

1001

1002 **Supplemental Tables**

1003 Table S1. The AC50 values of coumarin on HepG2 cells in references

1004 Table S2. The genes identified from HepG2 cells treated with different concentration of coumarin.

1005 Table S3. The proteins identified from HepG2 cells treated with different concentration of

1006 coumarin for 10 min.

1007 Table S4. The proteins identified from HepG2 cells treated with different concentration of

1008 coumarin for 24 hours.

1009 Table S5. The phosphosites identified from HepG2 cells treated with different concentrations of

1010 coumarin for 10 min.

1011 Table S6. The phosphosites identified from HepG2 cells treated with different concentration of

1012 coumarin for 24 hours.

1013 Table S7. The genes identified from AC16 cells treated with doxorubicin for different times.

1014 Table S8. The proteins identified from AC16 cells treated with doxorubicin for different times

1015    Table S9. The phosphosites identified from AC16 cells treated with doxorubicin for different

1016    times.

1017    Table S10. The number of 194 phosphosites (cluster 6) identified from AC16 cells treated with

1018    doxorubicin for different times.

1019    Table S11. The number of 157 proteins (match with 194 phosphosites) identified from AC16 cells

1020    treated with doxorubicin for different times.

1021    Table S12. The HMOX1 proteins identified from AC16 cells treated with doxorubicin for different

1022    times.

1023    Table S13. The phosphodites of TSC2 identified from AC16 cells treated with doxorubicin for

1024    different times.

1025    Table S14. The phosphodites of SQSTM1 identified from AC16 cells treated with doxorubicin for

1026    different times.

1027    Table S15. Parameter values of the mathematical model.

1028    Table S16. Ordinary differential equations (ODEs) of the mathematical model.